Vibrationally resolved predissociation of the $c\,^3\Pi_u$ and $e\,^3\Sigma_u^+$ states of H_2 by flight-time-difference spectroscopy*

B. Meierjohann and M. Vogler
2. Physikalisches Institut, Universität Giessen, 63 Giessen, Germany
(Received 18 July 1977)

The kinetic-energy distribution of H-H fragment pairs arising from dissociative charge-exchange collisions of 5-keV H_2^+ ions was measured using a flight-time-difference method. The spectrum exhibits 13 discrete kinetic energies between 7 and 10.5 eV in the center-of-mass frame of the projectile. Predissociation of the $c\,^3\Pi_u$ state by the repulsive $b\,^3\Sigma_u^+$ state explains most of the structure observed. In addition, evidence is found for predissociation of the $e\,^3\Sigma_u^+$ state.

I. INTRODUCTION

Radiationless transitions of a number of Rydberg states of molecular hydrogen into the dissociation continua of attractive Rydberg states of lower principal quantum number have been studied both experimentally and theoretically.[1] As a result of these predissociations, excited hydrogen atoms of small kinetic energies are produced.[2-6]

Very little is known, however, about the role played by the repulsive $b\,^3\Sigma_u^+$ state in predissociation of H_2. The first reference to the predissociation of the $c\,^3\Pi_u$ state by the $b\,^3\Sigma_u^+$ state was given by Lichten.[7] Herzberg[8] observed an anomalous intensity distribution in the absorption bands of H_2 excited by a flash discharge. He recognized predissociation of the $c\,^3\Pi_u$ state as the reason for this anomaly.

In contrast to the predissociation by attractive Rydberg states, the predissociation by the repulsive $b\,^3\Sigma_u^+$ state yields two ground-state atoms with an appreciable amount of kinetic energy. In a previous paper[9] we showed that discrete peaks in the kinetic-energy spectrum of H atoms arising from dissociative charge-exchange collisions of H_2^+ ions coincide very well with the energies of vibrational levels of the $c\,^3\Pi_u$ state above the dissociation limit of the electronic ground state. Since then, we have improved the resolution of our apparatus and found a large number of discrete peaks which we report in this paper.

II. EXPERIMENT

The excited H_2 molecules giving rise to predissociations are obtained in charge-exchange collisions of H_2^+ ions of approximately 5 keV incident on a static gas target. The H_2^+ ions are produced by a low-pressure electron impact ion source. The hydrogen pressure in the ion source is 2×10^{-3} Torr, the electron energy 100 eV, and the electron current about 4 mA. The ion source is water cooled. The solid angle subtended by the hot filament as seen from the ionization region is about 1% of the full 4π sr. Therefore, we assume that only a small fraction of the H_2 molecules have temperatures above room temperature. Since the yield of H_3^+ ions is about 1% as in von Busch and Dunn's experiment,[10] we expect the vibrational-level population of the H_2^+ ions to be that measured by von Busch and Dunn. The ions are accelerated, mass-analyzed, and fired through a collision chamber filled with hydrogen at 1×10^{-3} Torr. The collision chamber has a length of 1.5 cm.

The dissociation fragments arising from collisions of H_2^+ ions with target particles are detected by two detectors in coincidence with respect to their flight-time difference, flight direction, and charge. The distance between the collision chamber and the detectors is about 200 cm. The apparatus has been described in detail elsewhere.[11,12]

The principle of the flight-time-difference method is explained by means of Fig. 1. Let us assume $\vec{v}$ is a discrete velocity of fragment No. 1 relative to the center of mass of the H_2^+ ion. Then the corresponding velocity of fragment No. 2 is $-\vec{v}$. If we call the velocity of the center of mass in the laboratory frame after the collision $\vec{V}_{c.m.}$, then the velocities of both fragments in the laboratory frame, $\vec{V}_1$ and $\vec{V}_2$, are obtained by vectorial addition. Here $\vec{V}_{c.m.}$ is to a good approximation equal to the initial velocity of the H_2^+ ions for energies in the keV range, and v is much smaller than $V_{c.m.}$. Therefore, $\vec{V}_1$ and $\vec{V}_2$ are nearly parallel to each other and the angles between these vectors and $\vec{V}_{c.m.}$, Θ_1 and Θ_2, are nearly equal to each other. Let Θ be the mean of Θ_1 and Θ_2, i.e., $(\Theta_1+\Theta_2)/2=\Theta$. From Θ, $V_{c.m.}$, the flight-time difference of the two fragments, and the distance between the collision chamber and the two detectors, we derive v and the angle between v and the beam axis, ϑ. In the following,

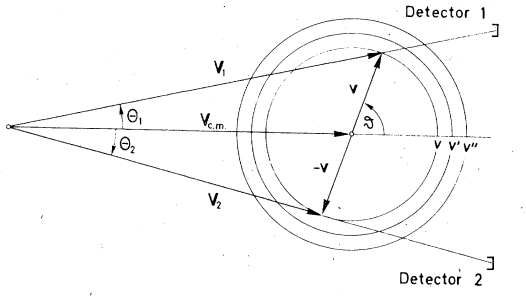

FIG. 1. Kinematic diagram for the collision-induced dissociation.

ϵ denotes the kinetic energy of both fragments in the center-of-mass frame, i.e., $\epsilon = mv^2$ (m is the proton mass).

Figure 1 shows two more discrete velocities v' and v''. At first sight, it does not seem to make any difference whether we measure at small Θ or large Θ in order to derive v. But since the separation between adjacent peaks in the flight-time-difference spectrum obviously increases when the angle Θ is increased, the velocity resolution can also be improved when the spectrum is taken at large Θ. Then, however, a better angular resolution is required. The entrance slits of the detectors were therefore reduced from 0.2 to 0.07 cm, thus limiting the angle of acceptance to 0.02°. Flight-time-difference spectra were then taken at the largest suitable angles.

III. RESULTS

The flight-time-difference spectra of H-H fragment pairs measured for three different pairs of H_2^+ energies and laboratory-frame scattering angles have been transformed into energy distributions in the center-of-mass frame.[11] The energy distributions shown in Fig. 2 give the number of H atoms flying into the solid-angle element $d\omega$ with respect to the center of mass of the H_2^+ ions when an energy between ϵ and $\epsilon + d\epsilon$ is released as kinetic energy of both fragments in the center-of-mass frame.

Plot (a) of Fig. 2 shows six pronounced peaks. Beyond 8.7 eV the time resolution is not sufficient to resolve any structure. As mentioned above, the energy resolution can be improved when the flight-time-difference spectra are recorded at larger angles Θ. This has been done in Fig. 2 (b). Here the three innermost peaks are already outside the range of velocities which can be recorded (compare Fig. 1). The energy resolution has clearly increased. Three more peaks appear. As far as plot (b) covers the energy range in which

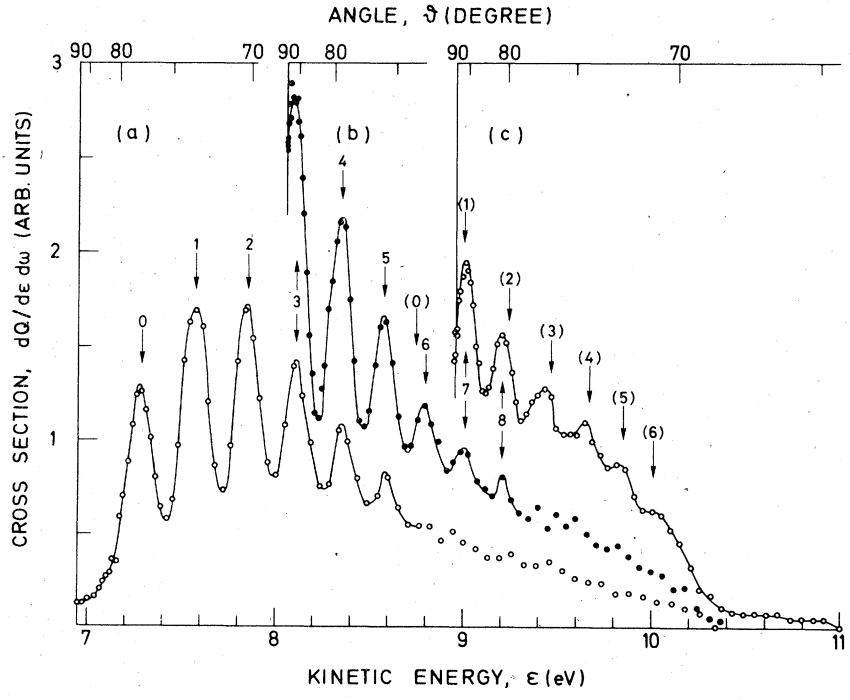

FIG. 2. Center-of-mass-frame energy distributions of H-H fragment pairs arising from collisional dissociation of H_2^+ ions incident on H_2. (a) H_2^+ energy $E = 5.243$ keV, lab-frame scattering angle $\Theta = 2.085°$; (b) $E = 5.243$ keV, $\Theta = 2.246°$; (c) $E = 5.826$ keV, $\Theta = 2.246°$. The center-of-mass-frame scattering angle ϑ changes with the kinetic energy ϵ. The peak sequence $0, 1, 2, \ldots, 8$ coincides with the energies of the vibrational levels of the $c\,^3\Pi_u$ state as far as known; the sequence $(0), (1), \ldots, (6)$ indicates the energies of the vibrational levels of the $e\,^3\Sigma_u^+$ state above the dissociation limit of the electronic ground state.

plot (a) also shows structure, there is an excellent agreement in the positions of the peaks.

Unfortunately, the angle Θ chosen for plot (b) could not be increased further in this high-resolution experiment. But the same effect of improving the resolution can be achieved when the H_2^+ energy is increased, because $V_{c.m.}$ gets larger and therefore Θ smaller. This has been done in Fig. 2(c). As a result four more peaks appear. There is again an excellent coincidence with the peaks already resolved in Fig. 2(b). Plot (c) then drops quickly to a low level at 10.4 eV before it reaches the abscissa at 11.0 eV.

The laboratory-frame scattering angles of the two fragments, Θ_1 and Θ_2, are not completely equal to each other. Their difference depends on the center-of-mass–frame scattering angle ϑ. This was taken into account by setting the two detectors slightly asymmetrically with respect to the beam axis, namely by 0.03°. If this is not done, a slight distortion of the intensity distribution occurs, favoring center-of-mass–frame scattering angles around $\vartheta = 90°$. The distortion depends on the angle of divergence of the primary H_2^+ beam and is smaller for larger divergence angles. Therefore, a less well collimated beam also helps to reduce this distortion. The angle of divergence can be increased by sweeping the H_2^+ beam as well.

On the top of Fig. 2 are given three different scales for the center-of-mass–frame scattering angles ϑ; ϑ changes with ϵ since the measurements were made at constant laboratory-frame scattering angles (compare Fig. 1). Moreover, the scales are different for the three plots. Each plot begins with $\vartheta = 90°$. Here the flight-time differences are zero. In principle, the curves plotted in Fig. 2 could be angle distributions as well as energy distributions, but a comparison of the three plots clearly shows that the peaks appear always at the same energies instead of at the same angles. Furthermore, the intensity ratio of adjacent peaks is the same in different plots. This shows that there is little anisotropy in the cross section.

The linearity of the energy scale is better than ± 0.02 eV; the absolute position of the whole energy scale is determined within ± 0.04 eV. The number of counts per channel is given approximately by the number on the ordinate times 1000. Thus, the statistical error is small. In order to achieve this accuracy it was necessary to accumulate data over 24 hours for curve (a), 2 days for curve (b), and one week for curve (c).

The curves were measured once more at half the pressure in the collision chamber with identical results.

IV. DISCUSSION

Figure 2 exhibits altogether 13 discrete peaks in the kinetic-energy spectrum of H-H fragment pairs between 7 and 10.5 eV. They are listed in Table I. The first nine peaks, numbered $0, 1, \ldots, 8$, form a series with continuously decreasing separations between successive peaks. The first four peaks of this series coincide within ± 0.02 eV with the energies of the lowest rotational levels of the $v = 0$ to $v = 3$ vibrational levels of the $c\ ^3\Pi_u$ state of H_2 above the dissociation limit of the electronic ground state (Table I). Therefore it is natural to assume that the remaining five peaks of this series belong to the $v = 4$ to $v = 8$ vibrational levels of this triplet state, too. The coordination applicable to our data is given in Table I.

As was shown by Lichten,[7] and later in more

TABLE I. Comparison of the observed energy levels with the energies of the vibrational levels of the c and e states above the dissociation limit of the electronic ground state after Dieke, as tabulated by Sharp (Ref. 13).

$c\ ^3\Pi_u$		$e\ ^3\Sigma_u^+$		Observed energy levels in eV	Vibrational-level coordination
v	E_v (eV)	v	E_v (eV)		
0	7.2859	(0)	8.7491	7.28	0
1	7.5762	(1)	9.0053	7.57	1
2	7.8513	(2)	9.2438	7.84	2
3	8.1109	(3)	9.4656	8.11	3
		(4)	9.6694	8.36	4
		(5)	9.8525	8.58	5
		(6)	10.0127	8.80	6
				9.01	7
				9.21	8
				9.43	9 + (3)
				9.65	(4)
				9.84	(5)
				10.03	(6)

detail by Herzberg,[8] the even rotational levels of the $c\,^3\Pi_u$ state of orthohydrogen and the odd rotational levels of parahydrogen can decay by allowed predissociations into the repulsive $b\,^3\Sigma_u^+$ state. Lichten estimated the lifetimes of these levels to be $\sim 10^{-9}$ sec.[7] We determined experimentally a lifetime of $\leq 10^{-8}$ sec.[9] While the $v=0$ vibrational level is known to be metastable with respect to decay by radiative dipole transitions,[14] transitions from higher vibrational levels into the $a\,^3\Sigma_g^+$ state can occur. Freis and Hiskes[15] found the radiative lifetimes of these levels to be of the order of 10^{-4} sec. Thus, the rates of predissociation are much faster than those of radiative dipole transitions.

The energy distributions shown in Fig. 2 should therefore reflect the populations of the vibrational levels in the $c\,^3\Pi_u$ state of H_2 formed here by charge-exchange collisions of H_2^+. Since the equilibrium distance of the two protons in the $c\,^3\Pi_u$ state is almost the same as in the electronic ground state of H_2^+, one can expect similar populations of the vibrational levels in both states. The profile formed by the peaks from $v=0$ to $v=6$ is indeed very similar to that obtained by von Busch and Dunn[10] for H_2^+. It should be mentioned that the energy distributions are not very sensitive to the target gas used as collision partner of the H_2^+ ions. Measurements with N_2 yielded very similar results.[16]

Two special features appear in the range above 9 eV. First, higher vibrational levels seem to be populated much more frequently in the $c\,^3\Pi_u$ state than in the H_2^+. Second, while the separations between successive peaks have decreased steadily up to $v=8$, they increase again before they decrease slightly once more. The peaks beyond $v=8$ do not move together to the degree one would expect if they belonged to the previous series.

The next higher electronic state which can decay by allowed predissociations into the $b\,^3\Sigma_u^+$ state is the $e\,^3\Sigma_u^+$ state. The energies of its vibrational levels above the dissociation limit of the electronic ground state are indicated by the numbers in brackets in Fig. 2 and are also listed in Table I. According to Kronig's selection rules[17] all hydrogen molecules in this state, not just half of them as in the $c\,^3\Pi_u$ state, can predissociate if there is a sufficient overlap of the vibrational wave functions of both states. In contrast to the predissociation of the $c\,^3\Pi_u$ state, which is almost without competition, the predissociation of the $e\,^3\Sigma_u^+$ state has to compete with decay by radiative dipole transitions into the $a\,^3\Sigma_g^+$ state. As a consequence, the cross section for predissociation of the $e\,^3\Sigma_u^+$ state in individual vibrational levels depends on the overlap integral between the $e\,^3\Sigma_u^+$ and $b\,^3\Sigma_u^+$ states. Since the two potential functions approach each other more closely for higher vibrational levels, we expect the maximum of the cross section for predissociation to be shifted towards higher vibrational levels. The dependence of the predissociation rate on the vibrational level has been observed by Herzberg[8] in the predissociation of the $c\,^3\Pi_u$ state.

Thus, in interpreting our spectra in the range above 8.7 eV we have to start from the fact that predissociation in the $e\,^3\Sigma_u^+$ state behaves differently from that in the $c\,^3\Pi_u$ state, and indeed in such a way that lower vibrational levels are weaker and higher levels are stronger. We assume that the levels $v=(0)$, (1), and (2) are weak and do not influence the positions of the nearby peaks $v=6$, 7, and 8 of the $c\,^3\Pi_u$ state. The position as well as the shape of the next peak suggests that it represents a superposition of the $v=9$ level of the $c\,^3\Pi_u$ state and the $v=(3)$ level of the $e\,^3\Sigma_u^+$ state, giving rise to a peak of some intermediate position. The last three peaks finally coincide very well with the energies of the $v=(4)$, (5), and (6) levels of the $e\,^3\Sigma_u^+$ state (Table I). The energy resolution would in any case not have been sufficient to resolve higher vibrational levels of the $c\,^3\Pi_u$ state in this range. We feel that the experimental evidence is strong enough to prove a contribution of the $e\,^3\Sigma_u^+$ state to the formation of hydrogen atoms of discrete kinetic energies by predissociation.

Beyond the $v=(6)$ peak the curve drops quickly to a low level before it reaches the abscissa at 11 eV. Although there seems to be some structure in this range, the intensity is too low to draw any conclusions on the contribution of any higher electronic states.

It should be stressed that predissociation of both the $c\,^3\Pi_u$ and $e\,^3\Sigma_u^+$ states makes only a small contribution to the total cross section for the production of hydrogen atom pairs in dissociative charge-exchange collisions of H_2^+ ions. Its proportion amounts to only 6% at a H_2^+ energy of 10 keV[18] and is of the same order of magnitude at 5 keV.

---

*Work supported by the Deutsche Forschungsgemeinschaft.

[1]P. M. Dehmer and W. A. Chupka, J. Chem. Phys. 65, 2243 (1976), and references given therein.

[2]M. Misakian and J. C. Zorn, Phys. Rev. A 6, 2180 (1972).

[3]L. Julien, M. Glass-Maujean, and J. P. Descoubes, J. Phys. B 6, L196 (1973).

[4]R. S. Freund, J. A. Schiavone, and D. F. Brader, J. Chem. Phys. 64, 1122 (1976).
[5]G. N. Polyakova, V. F. Yerko, A. I. Ranyuk, and O. S. Pavlichenko, Zh. Eksp. Teor. Fiz. 71, 1755 (1976) [Sov. Phys. JETP 44, 921 (1976).
[6]K. Ito, N. Oda, Y. Hatano, and T. Tsuboi, Chem. Phys. 17, 35 (1976); Chem. Phys. 21, 203 (1977).
[7]W. Lichten, Bull. Am. Phys. Soc. 7, 43 (1962).
[8]G. Herzberg, Sci. Light (Tokyo) 16, 14 (1967).
[9]M. Vogler and B. Meierjohann, Phys. Rev. Lett. 38, 57 (1977).
[10]F. von Busch and G. H. Dunn, Phys. Rev. A 5, 1726 (1972).
[11]B. Meierjohann and M. Vogler, J. Phys. B 9, 1801 (1976).
[12]B. Meierjohann and M. Vogler, Z. Phys. A 282, 7 (1977).
[13]T. E. Sharp, At. Data 2, 119 (1971).
[14]W. Lichten, Phys. Rev. 120, 848 (1960).
[15]R. P. Freis and J. R. Hiskes, Phys. Rev. A 2, 573 (1970).
[16]M. Vogler and B. Meierjohann, in *Abstracts of the Tenth International Conference on the Physics of Electronic and Atomic Collisions, Paris, 1977*, edited by M. Barat and J. Reinhardt (Commissariat a l'Energie Atomique, Paris, 1977), p. 568.
[17]See G. Herzberg, *Spectra of Diatomic Molecules* (Van Nostrand, Princeton, N. J. 1950), p. 416.
[18]M. Vogler and B. Meierjohann, Z. Phys. A 283, 11 (1977).